MOLECULAR PHYSICS, 2000, VOL. 98, NO. 5, 261–273

An accurate, global, *ab initio* potential energy surface for the H_3^+ molecule

OLEG L. POLYANSKY[1]†, RITA PROSMITI[1]‡, WIM KLOPPER[2]§ and JONATHAN TENNYSON[1]*

[1] Department of Physics and Astronomy, University College London, Gower St., London WC1E 6BT, UK

[2] Department of Chemistry, University of Oslo, PO Box 1033 Blindern, N-0315 Oslo, Norway

(*Received 30 September 1999; revised version accepted 25 October 1999*)

A new global, ground-state, Born–Oppenheimer surface is presented for the H_3^+ system. The energy switching approach has been used to combine different functional forms for three different regimes: a spectroscopic expansion at low energy, a Sorbie–Murrell function at high energy and known long-range terms combined with accurate diatomic potentials at large separations. At low energies we have used the ultra high accuracy *ab initio* data of Cencek *et al.* (1998, *J. chem. Phys.*, **108,** 2831). At intermediate energy we have calculated 134 new *ab initio* energies using a high accuracy, explicitly correlated procedure. The *ab initio* data of Schinke *et al.* (1980, *J. chem. Phys.*, **72,** 3909) has been used to constrain the high energy region. Two fits are presented which differ somewhat in their behaviour at energies over 45 000 cm^{-1} above the H_3^+ minimum. Below this energy, the fits reproduce each set of *ab initio* data close to their intrinsic accuracy. The ground state surface should provide a suitable starting point for renewed studies of the near-threshold photodissociation spectrum originally reported by Carrington *et al.* (1982, *Molec. Phys.*, **45,** 753).

1. Introduction

In this journal in 1982, Carrington *et al.* [1] gave a preliminary report of a truly remarkable photodissociation spectrum of the H_3^+ molecular ion. Carrington *et al.* observed some 27 000 clearly resolved photodissociation lines in a small, 222 cm^{-1}, region of the infrared. In subsequent work Carrington and co-workers [2, 3] provided further information on this spectrum. In particular they analysed the underlying course grained structure of the spectrum, the isotopomer specific behaviour displayed by H_2D^+ and D_2H^+, and the variation of the spectrum as a function of the kinetic energy release of the ionic fragment. The latter experimental analysis demonstrated that at least some of the spectrum arose from initial states which themselves are above the dissociation limit of the system. An overview of this work is provided by reviews of Carrington and McNab [4] and McNab [5].

The observations of Carrington *et al.* have stimulated considerable theoretical activity. Initially this work was largely (semi-)classical in nature [6–11], a review of which can be found in Pollak and Schlier [12]. One problem resolved by these studies was the reason for the observed isotope effect [6, 7]. More recently a number of studies have attempted to treat the problems raised by the H_3^+ photodissociation spectrum quantum mechanically [13–17]. However so far even the reason for the underlying coarse grained structure of the spectrum, the subject of greatest work, remains controversial [16]. A common feature of all these studies has been the use of potential energy functions which were either highly inaccurate or not designed for studies of the dissociation region.

Recently three of us (PPT) [18], in an attempt to address problems with the H_3^+ potential, developed a global two-valued ground-state potential surface for H_3^+, referred to below at the PPT surface. This surface used the energy switching functions of Varandas [19] to divide energy/configuration space into three regions: a low energy region which was represented by the Born–Oppenheimer portion of the spectroscopically deter-

* Author for correspondence. e-mail: j.tennyson@ucl.ac.uk

† Permanent address: Institute of Applied Physics Russian Academy of Science, Uljanov Street 46, Nizhnii Novgorod, Russia 603024.

‡ Present address: Department of Chemistry, University of Crete, Knossos Avenue, 71409 Heraklion, Crete, Greece.

§ Present address: Theoretical Chemistry Group, Debye Institute, Utrecht University, PO Box 80052, NL-3508 TB Utrecht, The Netherlands.

mined DPT potential of Dinelli *et al.* (DPT) [20], a high energy region characterized by the *ab initio* calculations of Schinke *et al.* [21] and a portion for large separations characterized by known long-range interaction terms and accurate diatomic potentials.

The PPT potential is reliable for a large range of H_3^+ geometries including the entire dissociation region and the region where the two surfaces cross; however the PPT surface cannot be regarded as accurate. In particular the use, in the absence of better data, of the 1980 *ab initio* data of Schinke *et al.* meant that it was not possible for Prosmiti *et al.* to obtain high accuracy. Subsequent to this work Cencek *et al.* [22] reported the ultra high accuracy ('sub-microhartree') *ab initio* calculation in the low energy region of the potential. We have therefore undertaken further *ab initio* calculations which allow us to characterize a global, high accuracy surface. It is this work which we report here.

2. Electronic structure calculations

The input to determine our potential energy surface came from a number of different *ab initio* electronic structure calculations. To balance our fits it is therefore necessary to weight these points according to their accuracy.

At low energy we use the 69 potential energy points computed by Cencek *et al.* [22] at the grid points originally suggested by Meyer *et al.* (MBB) [23]. These energies have an absolute accuracy of about $0.05\,cm^{-1}$.

Our aim here is to construct a potential surface on which H_3^+ can dissociate. However, to constrain our fit at high energies we use the *ab initio* data of Schinke *et al.* [21]. Schinke *et al.* computed energies at 650 grid points with boundaries $0.0\,a_0 \leqslant R \leqslant 10.0\,a_0$, $0.6\,a_0 \leqslant r \leqslant 2.6\,a_0$ and $0^\circ \leqslant \theta \leqslant 90^\circ$ in Jacobi coordinates. In these coordinates, r is the H–H distance, R is the distance between H^+ and the centre of mass of H_2, and θ is the angle between **r** and **R**. We estimate the accuracy of Schinke *et al.*'s energies to be about $300\,cm^{-1}$, by comparison with the data of Cencek *et al.* [22]. Unlike PPT, our fits used all 492 of Schinke *et al.*'s points lying below $75\,000\,cm^{-1}$.

To characterize the potential at intermediate energies, we have computed non-relativistic Born–Oppenheimer electronic energies on 134 points on the potential energy hyper-surface of the H_3^+ ion. These cover energies up to $70\,000\,cm^{-1}$ above the minimum of the potential. These points, which are listed with our calculated electronic energies in table 1, were chosen by extending the MBB [23] grid employed by Cencek *et al.*, choosing those points which, according to the PPT potential, lay at low energy. The MBB grid uses displacements from equilibrium in symmetry coordinates; in table 1 we have converted these to Jacobi coordinates for ease of interpretation. In this context it should be noted that none of our newly calculated points lie in the region of the $r \sim 2.5\,a_0$ and $R \geqslant 8\,a_0$ in which the surface crossing is important [18].

Our electronic structure calculations employed the CISD-R12 method of Kutzelnigg and co-workers [24–26]—the same method used in previous accurate computations of the H_3^+ surface [27, 28]. In the CISD-R12 method, the electronic wavefunction is approximated as

$$\Psi(1,2) = r_{12}\Phi_0(1,2) + \sum_{k=0}^{N} c_k \Phi_k(1,2), \qquad (1)$$

where r_{12} is the inter-electronic distance and $\Phi_k(1,2)$ the two-electron basis set of all N singlet Slater determinants that can be built from a contracted 10s8p6d4f Gaussian basis set of atomic orbitals (AOs). The 10s8p6d4f AO basis set used here was obtained by contracting the 16s10p8d6f primitive basis set of [27, 28]. The contraction coefficients were obtained from a calculation on the bare nuclear Hamiltonian of the equilateral triangular H_3^+ ion with internuclear separation $r = 1.65\,a_0$, as explained in [27]. The CISD-R12 energy of the H_3^+ ion in this geometry amounts to $-1.343\,8341\,E_h$; this can be compared to the value of $-1.343\,8355\,E_h$, $0.3\,cm^{-1}$ lower, obtained by Cencek *et al.* [22] for the same geometry.

The reference wavefunction $\Phi_0(1,2)$ is the singlet two-electron Slater determinant that is built from the molecular orbital corresponding to the lowest eigenvalue of the above-mentioned bare nuclear Hamiltonian. All calculations were performed with the DIS program [29] on the SGI/CRAY Origin 2000 of the University of Bergen, Norway.

For the set of points ($N_a = -4, -3, \ldots, 4, 5$, $N_x = 0$, $N_y = 0$) computed by Cencek *et al.* [22], our present calculations deviate from their surface by at most $0.5\,cm^{-1}$, see table 2. Noting that this deviation increases in a regular manner with the distance from the equilibrium structure, we expect deviations of about $1\,cm^{-1}$ for the energy points around $50\,000\,cm^{-1}$ above the minimum. For example, we predict an error of $0.9\,cm^{-1}$ for the energy point ($N_a = -6$, $N_x = 0$, $N_y = 0$), which lies $48\,662.9\,cm^{-1}$ above the minimum in our new calculations. However it should be noted that the present method of computation is not strictly variational and, as can be seen from table 2, energies can be too low as well as too high.

For the whole set of 133 new *ab initio* points† computed by us, we estimate—rather conservatively—an average accuracy of $3\,cm^{-1}$, which is three times larger than the maximum error predicted for the calculations

† The first point serves only to define the energy zero.

Table 1. Born–Oppenheimer electronic energies, relative to the first point at $-1.343\,834\ E_h$. Geometries are defined in Jacobi coordinates. Residues for the fit are given in cm^{-1}.

					$E - V_{ES}$	
No.	r/a_0	R/a_0	$\cos\theta$	E/cm^{-1}	Fit 1	Fit 2
1	1.650 00	1.428 94	0.000 00	0.00	0.09	0.09
2	0.994 94	0.861 64	0.000 00	48 662.89	7.08	7.22
3	0.936 02	0.920 92	0.221 58	51 838.50	2.61	2.89
4	1.219 59	0.855 15	0.368 45	43 747.57	9.40	10.19
5	1.149 57	0.889 53	0.195 46	34 703.18	−6.23	−2.75
6	1.083 22	0.938 10	0.000 00	31 849.09	−2.78	−5.90
7	1.020 16	1.001 94	0.218 49	34 543.56	4.47	6.35
8	1.492 75	0.901 91	0.637 12	63 822.46	−13.51	−44.91
9	1.325 70	0.931 81	0.364 15	29 342.52	3.48	5.23
10	1.045 90	1.177 97	0.460 36	28 377.97	−0.88	−2.69
11	0.984 63	1.289 28	0.736 63	39 563.22	−7.61	−22.06
12	1.530 27	0.992 11	0.508 50	30 324.60	−12.60	−8.28
13	1.072 18	1.408 03	0.742 14	27 911.82	−7.32	−10.36
14	1.774 27	1.075 93	0.630 38	35 978.76	1.24	17.97
15	2.226 53	1.226 48	0.810 69	68 307.73	−1.66	−5.61
16	1.942 54	1.176 98	0.631 94	27 846.27	0.52	0.55
17	2.294 22	1.314 13	0.736 56	37 135.51	−7.01	−10.26
18	2.557 03	1.457 24	0.746 13	32 351.27	−13.11	−26.27
19	3.190 09	1.731 89	0.838 59	43 187.17	7.16	37.90
20	2.888 85	1.632 80	0.761 73	30 250.48	2.58	4.94
21	4.510 69	2.347 38	0.920 78	53 133.97	−3.78	−2.90
22	3.339 37	1.863 76	0.785 68	30 514.57	5.86	7.27
23	4.989 17	2.619 68	0.903 30	39 810.14	9.41	10.23
24	4.044 21	2.213 44	0.823 03	32 816.02	−3.88	−5.01
25	3.508 57	2.025 87	0.721 51	26 511.72	11.41	12.51
26	5.766 28	3.044 70	0.892 39	36 174.31	0.86	1.48
27	4.355 47	2.441 00	0.777 78	32 651.81	−1.15	−1.38
28	3.703 85	2.232 47	0.641 57	28 551.52	1.51	2.52
29	3.275 39	2.166 50	0.472 43	25 242.08	−8.52	−8.49
30	2.306 21	3.288 57	0.900 01	26 314.22	−0.09	−1.05
31	4.768 75	2.747 24	0.725 78	38 153.35	10.71	24.03
32	3.934 73	2.512 77	0.535 81	35 037.15	0.35	0.16
33	3.435 73	2.501 62	0.301 93	32 955.60	−0.04	−1.57
34	3.078 48	2.666 04	0.000 00	32 241.38	7.16	7.23
35	2.800 01	3.114 66	0.438 14	33 084.67	1.10	3.41
36	5.385 52	3.203 81	0.665 84	47 953.22	−2.69	−7.09
37	4.217 17	2.945 25	0.375 49	45 131.01	−2.39	9.66
38	3.619 29	3.134 40	0.000 00	44 257.50	5.82	−19.59
39	3.214 49	4.133 42	0.702 61	45 297.34	−0.72	−3.43
40	0.975 91	1.033 98	0.132 65	34 623.36	−0.61	2.07
41	1.062 84	1.123 81	0.131 79	21 657.53	0.69	0.69
42	1.156 16	1.221 59	0.131 94	12 342.85	0.53	0.53
43	1.256 89	1.328 87	0.133 20	6124.06	0.41	0.42
44	1.366 30	1.447 67	0.135 72	2563.87	0.02	0.01
45	1.486 05	1.580 78	0.139 82	1320.62	−0.01	−0.03
46	1.618 28	1.732 09	0.145 95	2133.12	0.12	0.11
47	1.765 91	1.907 38	0.154 93	4811.61	0.06	0.08
48	1.933 01	2.115 63	0.168 19	9234.99	0.08	0.07
49	2.125 48	2.372 14	0.188 52	15 356.34	0.02	0.02
50	2.352 44	2.706 25	0.222 23	23 222.25	0.74	0.88
51	2.629 03	3.187 05	0.287 42	33 020.20	−0.11	−2.28
52	2.983 18	4.073 89	0.470 84	45 209.07	−1.82	−4.49

Continued

Table 1. *Continued*

No.	r/a_0	R/a_0	$\cos\theta$	E/cm^{-1}	$E - V_{ES}$ Fit 1	$E - V_{ES}$ Fit 2
53	0.957 17	1.228 85	0.298 57	28 859.76	4.13	3.89
54	1.042 78	1.336 58	0.300 04	18 512.37	1.23	1.31
55	1.134 58	1.455 86	0.304 52	11 443.00	0.48	0.49
56	1.233 54	1.589 50	0.312 60	7177.19	0.42	0.45
57	1.340 88	1.741 43	0.325 28	5345.99	0.22	0.23
58	1.458 14	1.917 49	0.344 27	5668.93	0.12	0.17
59	1.587 34	2.126 94	0.372 60	7944.57	0.43	0.43
60	1.731 21	2.385 79	0.416 21	12 049.95	1.05	0.86
61	1.893 49	2.725 95	0.488 44	17 954.88	3.34	3.52
62	2.079 61	3.229 25	0.627 91	25 774.84	3.38	3.65
63	0.938 70	1.459 92	0.519 21	29 114.22	−7.05	−10.53
64	1.023 03	1.594 15	0.530 16	20 576.08	0.59	0.60
65	1.113 36	1.746 96	0.548 99	15 102.76	0.26	0.15
66	1.210 62	1.924 49	0.578 40	12 278.89	0.55	0.54
67	1.315 95	2.136 64	0.623 25	11 794.78	2.35	2.58
68	1.430 82	2.401 14	0.693 16	13 440.81	0.73	0.73
69	1.557 14	2.755 33	0.810 13	17 124.45	5.62	5.69
70	0.769 05	1.462 87	0.799 92	59 497.19	11.80	49.74
71	0.920 49	1.752 63	0.833 82	33 962.46	−3.93	−16.80
72	1.003 58	1.932 85	0.873 15	26 734.75	−4.83	−3.54
73	1.092 49	2.149 79	0.935 64	22 506.46	0.74	0.74
74	1.129 78	0.978 42	0.000 00	25 085.98	13.40	12.84
75	1.178 11	1.020 27	0.000 00	19 294.82	0.48	0.49
76	1.228 35	1.063 78	0.000 00	14 395.59	−1.25	−1.38
77	1.280 67	1.109 09	0.000 00	10 317.16	0.41	0.40
78	1.335 23	1.156 35	0.000 00	6996.33	0.67	0.73
79	1.392 25	1.205 72	0.000 00	4376.93	0.15	0.17
80	1.451 95	1.257 42	0.000 00	2409.10	−0.02	−0.05
81	1.514 59	1.311 68	0.000 00	1048.78	0.10	0.07
82	1.580 49	1.368 75	0.000 00	257.08	0.14	0.13
83	1.723 54	1.492 63	0.000 00	248.03	0.06	0.05
84	1.801 60	1.560 23	0.000 00	975.95	0.09	0.08
85	1.884 78	1.632 26	0.000 00	2162.70	0.04	0.03
86	1.973 79	1.709 35	0.000 00	3791.32	−0.16	−0.17
87	2.069 52	1.792 26	0.000 00	5848.98	−0.31	−0.33
88	2.173 07	1.881 93	0.000 00	8327.21	−0.08	−0.08
89	2.285 81	1.979 57	0.000 00	11 222.21	0.38	0.40
90	2.409 56	2.086 74	0.000 00	14 535.40	0.08	0.09
91	2.546 69	2.205 50	0.000 00	18 274.30	0.02	−0.07
92	2.700 45	2.338 66	0.000 00	22 453.50	−0.02	−0.02
93	2.875 45	2.490 21	0.000 00	27 097.33	−28.40	−27.85
94	3.320 30	2.875 46	0.000 00	37 937.14	−8.66	−1.61
95	0.923 33	1.443 35	0.260 04	27 671.18	7.60	8.04
96	0.944 27	1.921 89	0.545 72	29 270.35	4.43	2.32
97	0.968 50	2.156 91	0.154 05	29 009.13	5.34	6.36
98	1.054 90	2.398 28	0.171 26	25 603.34	3.91	5.95
99	1.147 62	2.699 62	0.199 54	24 694.77	2.65	4.41
100	1.247 65	3.100 24	0.250 79	26 052.48	−0.64	−1.86
101	1.669 63	3.022 53	0.490 93	20 975.32	−8.02	−9.55
102	1.356 24	3.699 21	0.365 55	29 545.10	5.36	5.11
103	2.187 86	2.884 55	0.191 87	23 916.37	1.51	1.72
104	1.000 76	1.176 87	0.103 67	24 157.61	2.62	2.60
105	0.962 82	1.616 29	0.245 85	23 220.62	0.84	0.79

Continued

Table 1. *Continued*

No.	r/a_0	R/a_0	$\cos\theta$	E/cm^{-1}	$E - V_{ES}$ Fit 1	$E - V_{ES}$ Fit 2
106	1.012 49	2.144 33	0.583 82	25 774.36	2.69	1.56
107	1.102 05	2.393 85	0.647 20	23 172.55	10.17	8.42
108	1.198 41	2.714 87	0.752 15	23 052.75	−7.00	−9.79
109	1.302 70	3.171 26	0.948 09	25 338.92	0.83	0.59
110	1.596 65	3.142 64	0.483 72	22 452.87	0.57	−2.77
111	2.187 86	2.884 55	0.191 87	23 916.37	1.51	1.72
112	1.625 72	0.984 88	0.632 19	47 730.02	18.33	26.96
113	4.011 16	3.473 76	0.000 00	51 303.88	−0.23	9.87
114	3.056 54	1.622 13	0.882 50	68 962.27	4.24	−13.34
115	3.794 45	2.034 66	0.862 46	40 684.92	16.04	35.75
116	0.894 56	0.950 91	0.134 47	51 945.08	−11.70	−12.48
117	1.056 72	0.816 16	0.198 71	52 051.55	−26.93	−28.76
118	0.879 72	0.995 18	0.468 28	61 103.21	21.08	30.07
119	1.293 69	0.834 11	0.518 49	60 030.88	−61.56	−85.49
120	0.960 09	1.082 67	0.462 59	42 435.63	128.64	129.89
121	0.902 74	1.182 80	0.737 82	55 396.92	291.23	322.41
122	1.406 48	0.910 01	0.512 17	42 964.62	−45.51	−39.31
123	2.474 26	1.360 01	0.814 81	56 387.90	−36.47	−5.98
124	2.782 37	1.522 33	0.823 64	48 224.66	−39.84	−4.04
125	6.312 75	3.208 12	0.967 61	68 820.90	−222.65	1330.70
126	6.632 82	4.082 45	0.603 04	60 136.71	−246.69	−246.69
127	4.581 00	3.967 26	0.000 00	59 210.79	−3945.31	−3196.47
128	0.876 97	1.130 64	0.299 79	43 090.88	67.44	67.91
129	0.859 62	1.340 18	0.514 64	41 258.00	−45.26	−59.70
130	0.842 51	1.598 18	0.810 65	44 669.11	−102.54	−88.21
131	1.038 31	0.899 20	0.000 00	39 674.21	48.78	52.99
132	1.890 90	1.086 40	0.730 85	56 565.49	79.99	87.39
133	2.076 61	1.192 54	0.731 72	45 021.00	46.65	67.57
134	8.129 39	4.238 72	0.917 01	39 517.43	36.86	28.85

Table 2. Comparison of Born–Oppenheimer electronic energies for the present calculation and that of Cencek *et al.* [22]. Calculations are for equilateral triangular H_3^+ with internuclear separation r. Energies, in cm^{-1}, are relative to the $r = 1.65\,a_0$ point for each calculation.

r/a_0	[22]	This work	Δ
1.1781	19294.33	19294.82	+ 0.49
1.2807	10316.83	10317.16	+ 0.33
1.3922	4376.74	4376.93	+ 0.19
1.5146	1048.70	1048.78	+ 0.08
1.8016	975.99	975.95	−0.04
1.9738	3791.37	3791.32	−0.05
2.1731	8327.24	8327.21	−0.03
2.4096	14535.39	14535.40	+ 0.01
2.7005	22453.63	22453.50	−0.13

on the equilateral triangular geometries. The fitted potentials below reproduce the computed data in the energy range of our new points with a standard deviation of around $5\,cm^{-1}$ for points which lie below $39\,000\,cm^{-1}$. Thus, the standard deviation of the fit is of the same order of magnitude as the intrinsic accuracy of the *ab initio* calculations.

3. Analytical representation of the PES

As the functional form employed by Prosmiti *et al.* [18] to represent their two-valued, global ground state potential function gave physically reasonable values for all the configurations we wish to consider, we used this as a starting point for our representation of the potential. The PPT potential used a combination of two potential forms, $V_1(\mathbf{R})$ and $V_2(\mathbf{R})$, linked by the energy switching approach of Varandas [19]. Within this approach, V_2 reproduces the low energy 'spectroscopic' portions of the potential in the region of the minimum of the potential. V_1 should give a realistic representation for configurations at higher energies. The energy switching (ES) potential is written as

$$V_{\mathrm{ES}} = f^{+}(\Delta E)V_1(\mathbf{R}) + f^{-}(\Delta E)V_2(\mathbf{R}), \qquad (2)$$

where $f(\Delta E)$ is the switching function with the general form [19]

$$f^{\pm}(\Delta E) = \tfrac{1}{2}[1 + \tanh(\pm\gamma\Delta E)] \qquad (3)$$

and

$$\gamma = \gamma_0 + \gamma_1\Delta E^2, \qquad \Delta E = E - E_0. \qquad (4)$$

Initially we used values of the switching parameters γ_0, γ_1 and E_0 as PPT. In contrast to PPT, the value of E used to determine ΔE was taken from the V_1 potential.

The low energy 'spectroscopic' part of the potential, V_2, was expressed in symmetry coordinates:

$$S_a = (\tilde{R}_{12} + \tilde{R}_{23} + \tilde{R}_{31})/3^{1/2},$$

$$S_x = (2R_{12} - R_{23} - R_{31})/6^{1/2} = S_{\mathrm{e}}\cos(\phi),$$

$$S_y = (R_{23} - R_{31})/2^{1/2} = S_{\mathrm{e}}\sin(\phi). \qquad (5)$$

Following high accuracy fits to this region of the potential [30], the distortions were represented using simple displacement coordinates: R_{jk} is the distance between atom j and atom k. The (dissociative) breathing mode was represented using Morse coordinates

$$\tilde{R}_{jk} = \left[1 - \exp\left(-\beta\frac{R_{jk} - R_{\mathrm{e}}}{R_{\mathrm{e}}}\right)\right] \Big/ \beta, \qquad (6)$$

where R_{e} is the equilibrium separation which was assumed to be $1.65\,a_0$ and the Morse parameter β was fixed at 1.3 [23].

In these coordinates the V_2 potential was expanded as a polynomial where

$$V_2 = \sum_{n,m,k} V_{n,m,k} S_a^n S_{\mathrm{e}}^{m+k}\cos(k\phi),$$

$$m = 0,2,4,\ldots, \quad k = 0,3,6,\ldots, \qquad (7)$$

where $N \geqslant n + m + k$ gives the order of the fit. As this portion of the potential is largely determined by the *ab initio* data of Cencek *et al.* [22], V_2 was initially set to the tenth-order fit of Polyansky and Tennyson [30], which reproduces Cencek *et al.*'s data with a standard deviation of $0.04\,\mathrm{cm}^{-1}$.

The V_1 surface was represented by the Sorbie–Murrell [31] many body expansion form. This representation of the PES for H_3^+ is a three-valued surface [32], taking into account all the dissociation schemes. In this approach, the two-body terms are the potential curves of the ground H_2, H_2^+ and the first excited state of H_2^+. The repulsive state of H_2^+ lies above the H+ H^+ + H limit, so can safely be neglected. We therefore copy PPT who followed Carter [32] and construct an approximate two-valued surface of H_3^+, by considering two diabatic states V_{aa} and V_{bb}, which correspond to the dissociation channels H_2+ H^+ and H_2^+ + H respectively. In this two-valued representation, the ground and first excited states of H_3^+ are the eigenvalues of a 2×2 matrix. The lowest eigenvalue is given by

$$V_1 = \tfrac{1}{2}[V_{aa} + V_{bb} - [(V_{aa} - V_{bb})^2 + V_{ab}^2]^{1/2}]. \qquad (8)$$

The diabatic surfaces are given by the forms,

$$V_{aa} = V_{\mathrm{HH}}^{(2)}(R_1) + V_{\mathrm{HH}}^{(2)}(R_2) + V_{\mathrm{HH}}^{(2)}(R_3) + V_{aa}^{(3)}(R_1,R_2,R_3), \qquad (9)$$

$$V_{bb} = V_{\mathrm{HH}^+}^{(2)}(R_1) + V_{\mathrm{HH}^+}^{(2)}(R_2) + V_{\mathrm{HH}^+}^{(2)}(R_3) + V_{bb}^{(3)}(R_1,R_2,R_3), \qquad (10)$$

where R_1, R_2, R_3 are the bond lengths of the three possible diatomic products. $V^{(2)}$ are the two-body terms and $V^{(3)}$ are the three-body terms, which are constructed with full permutation symmetry. Parameters for the two-body terms were determined by PPT using the very high accuracy *ab initio* data of Bishop and Shih [33] for H_2, and Schwartz and Le Roy [34] for H_2^+. These were used here.

The most important short-range (SR) three-body term is $V_{aa}^{(3)\mathrm{SR}}$. This was represented as a 7th order polynomial

$$V_{aa}^{(3)\mathrm{SR}} = P(R_1,R_2,R_3)T(R_1,R_2,R_3) \qquad (11)$$

$$P(R_1,R_2,R_3) = V_0\Bigg(1 + \sum_{i=1}^{3} C_i\rho_i + \sum_{i\leqslant j}^{3} C_{ij}\rho_i\rho_j + \sum_{i\leqslant j\leqslant k}^{3} C_{ijk}\rho_i\rho_j\rho_k + \sum_{i\leqslant j\leqslant k\leqslant l}^{3} C_{ijkl}\rho_i\rho_j\rho_k\rho_l + \sum_{i\leqslant j\leqslant k\leqslant l\leqslant n}^{3} C_{ijkln}\rho_i\rho_j\rho_k\rho_l\rho_n + \sum_{i\leqslant j\leqslant k\leqslant l\leqslant n\leqslant m}^{3} C_{ijklnm}\rho_i\rho_j\rho_k\rho_l\rho_n\rho_m + \sum_{i\leqslant j\leqslant k\leqslant l\leqslant n\leqslant m\leqslant z}^{3} C_{ijklnmz}\rho_i\rho_j\rho_k\rho_l\rho_n\rho_m\rho_z\Bigg) \qquad (12)$$

$$T(R_1,R_2,R_3)=\prod_{i=1}^{3}\left[1-\tanh\left(\frac{g_i\rho_i}{2}\right)\right],$$

$$\rho_i=R_i-R_0,\quad i=1,2,3. \tag{13}$$

Initial parameters for $V_{aa}^{(3)\mathrm{SR}}$ were determined by fitting to our newly calculated data. The form of $V_{ab}^{(3)}$ and $V_{bb}^{(3)}$ were taken unchanged from PPT throughout the fit as the *ab initio* data we introduce here contains no new information on these terms.

The functional form used to represent the three-body terms does not display the correct behaviour when one atom/ion is well separated from the other two. To describe the charge-induced dipole and charge-quadrupole contributions we introduced long-range (LR) values known from perturbation theory [35]. This leads to revised three-body terms given by:

$$V_{aa}^{(3)}=g(R)V_{aa}^{(3)\mathrm{SR}}+[1-g(R)]V_{aa}^{\mathrm{LR}} \tag{14}$$

with the switching function defined by

$$g(R)=\begin{cases}1, & R<R_{LIM},\\ \cos^2\left[\dfrac{\pi(R-R_{LIM})}{2(R_M-R_{LIM})}\right], & R_{LIM}\leqslant R\leqslant R_M,\\ 0, & R>R_M.\end{cases} \tag{15}$$

PPT used a long-range potential and switching functions based on one, arbitrary, definition of the Jacobi coordinate. This results in a potential which, for certain geometries, does do not reflect the full symmetry of this system. For this reason we chose R in V^{LR} and $g(R)$ using the minimum H–H distance to define r in the three possible choices of Jacobi coordinates. This has the effect of symmetrizing the long-range part of the potential although it is possible that such a potential will display a cusp in regions where the definition of R is swapped. We have detected no problems with cusp-like behaviour in the potentials reported below.

For $V_{aa}^{(3)}$ PPT defined the switching region by $R_{LIM}=4.0\,\mathrm{a_0}$ and $R_M=10.0\,\mathrm{a_0}$. However, we found that at large values of R, $V_{aa}^{(3)\mathrm{SR}}$ introduced structure into the potential. As there is no data defining $V_{aa}^{(3)\mathrm{SR}}$ at large R these features must be regarded as artificial; they were removed by resetting R_M to $7.0\,\mathrm{a_0}$. The functional form for the upper diabatic state the V_{bb}^{LR} and the parameters for the long-range (LR) terms were taken from PPT.

Unlike PPT who determined V_1 and V_2 separately our fits were performed for the entire surface. To avoid problems with excessive correlations, we alternated between varying the parameters for each portion of the potential.

As we are using *ab initio* data from three different sources it is necessary to define a common energy zero and to weight the data according to its approximate accuracy. The energy zero was fixed for each data set by defining the potential of the equilateral triangle geometry with $r=1.65\,\mathrm{a_0}$ to be zero. The weighting used in the fits was not an absolute error but a relative one. Our final fits weighted the error of our calculations as 60 times less than, and Schinke *et al.*'s as 19 760 times less than, those of Cencek *et al.* Our calculations gave a few points at relatively high energy. It was found that there were too few of these for them to be fitted accurately, so 18 points, listed last in table 1, were dropped from our fits. Thus, if one assumes that the 69 points of Cencek *et al.* are accurate to $0.05\,\mathrm{cm^{-1}}$, then this weights our 115 points with an accuracy of $3\,\mathrm{cm^{-1}}$, and Schinke *et al.*'s 650 points with an accuracy of $988\,\mathrm{cm^{-1}}$. The low weighting of the data of Schinke *et al.* was because this data was used merely to constrain the surface to physically reasonable values in regions where no other information is available.

Initially we used PPT's values for the switching function, $f^{\pm}(\Delta E)$. Introducing our new data allowed us to determine further parameters in V_2. These were introduced until all parameters up to twelfth-order were included in the fit. A large number of iterations were then performed to obtain optimum parameters for both V_1 and V_2. The more difficult fits, namely those for V_1 which are nonlinear, were performed using the sophisticated interactive nonlinear least squares (I-NoLLS) [36] program. For the linear V_2 fits, a much simpler fitting program was sufficient.

The result of this fit reproduced our input data reasonably satisfactorily but inspection of the resulting potential showed that there was a problem with unphysical holes in what should have been the high energy region. Analysis showed that this problem was due to large oscillations in V_2 outside its domain of validity. To cure this problem we investigated changing the parameters in the switching function, $f^{\pm}(\Delta E)$. Essentially these are of two types: the parameter E_0 where the switching occurs and the parameter γ determines how fast the switching occurs. As our new data leads to V_2 being determined to significantly higher energies than the DPT potential used by PPT to define V_2, we decided to raise E_0. Conversely the unphysical holes were caused by the switching being too soft allowing V_2 to influence regions of the potential where it was not well determined. We therefore decided to sharpen the switch over by increasing γ_2. There is a certain arbitrariness in this procedure and in practice we found little sensitivity in our fits once γ_2 was raised above a certain value. We therefore chose a value of γ_2 at the low end of this

range so as not too make the switch over excessively sharp.

Use of the new switching function not only removed problems with the artificial holes in the potential, it also gave an improved representation of our data. We used this as a starting point for more iterations fitting alternatively V_1 and V_2. This yielded a further significant improvement in the fit of our data. However graphical analysis of our potential showed that our changes to $f^{\pm}(\Delta E)$ had introduced another problem: as the switching energy was raised, V_2 was now found to make a small but significant contribution in the long-range region. As discussed above, PPT only matched the three-body terms in V_1 to the correct long-range functions. We found it was necessary to treat V_2 in a similar fashion and generalize its definition:

$$\tilde{V}_2 = g(R)V_2 + [1 - g(R)](V_{aa}^{\mathrm{LR}} + V_{\mathrm{HH}}^{(2)}(r) - V_{\mathrm{HH}}^{(2)}(r_{\mathrm{e}}) + D_{\mathrm{e}}), \quad (16)$$

where $g(R)$ is the switching function as defined in (15) using $R_{LIM} = 4.5\,\mathrm{a_0}$ and $R_M = 10.0\,\mathrm{a_0}$; $V_{\mathrm{HH}}^{(2)}$ is the H_2 potential curve of Bishop and Shih [33] used above. The energy zeroes are made consistent by setting the energy $V_{\mathrm{HH}}^{(2)}$ to zero for at the H_2 equilibrium bond length, r_{e} and setting D_{e} to the dissociation energy of H_3^+. For D_{e} we used the best available *ab initio* value of Röhse *et al.* [28] of $37\,170.4\,\mathrm{cm^{-1}}$. This is the same value of D_{e} that was used by PPT, and hence us, in parametrizing V_1. It should be noted that the best experimentally determined dissociation energy of H_3^+ is about $320\,\mathrm{cm^{-1}}$ higher than this [37] and that the theoretical ($\pm 0.5\,\mathrm{cm^{-1}}$) and experimental ($\pm 20\,\mathrm{cm^{-1}}$) error bars means that these values are incompatible with each other.

After performing further iterations using $\tilde{V}_2$ in the potential we obtained our best fit to the input data, which we call Fit 1 below. Fit 1 reproduces all Cencek *et al.*'s data with a standard deviation of $0.059\,\mathrm{cm^{-1}}$. It reproduces the 115 of our electronic structure used in the fit with a standard deviation of $5.8\,\mathrm{cm^{-1}}$. Table 1 gives individual residues for these newly calculated points, including those not included in the fit. Schinke *et al.*'s data was fitted with a standard deviation of $535\,\mathrm{cm^{-1}}$.

It is difficult to prove that a potential hyper-surface is smooth everywhere and contains no unphysical regions. Besides analysing the various residuals of our fits, we also inspected plots of the potential, see figure 1 (*a*) for example. These plots showed the potential to be smooth but also suggested that the result of this fit, Fit 1, was to produce a 'shoulder' in the potential for some near-linear geometries for $50\,000\,\mathrm{cm^{-1}}$ and above. This feature was not present in the PPT potential and appears to be unphysical.

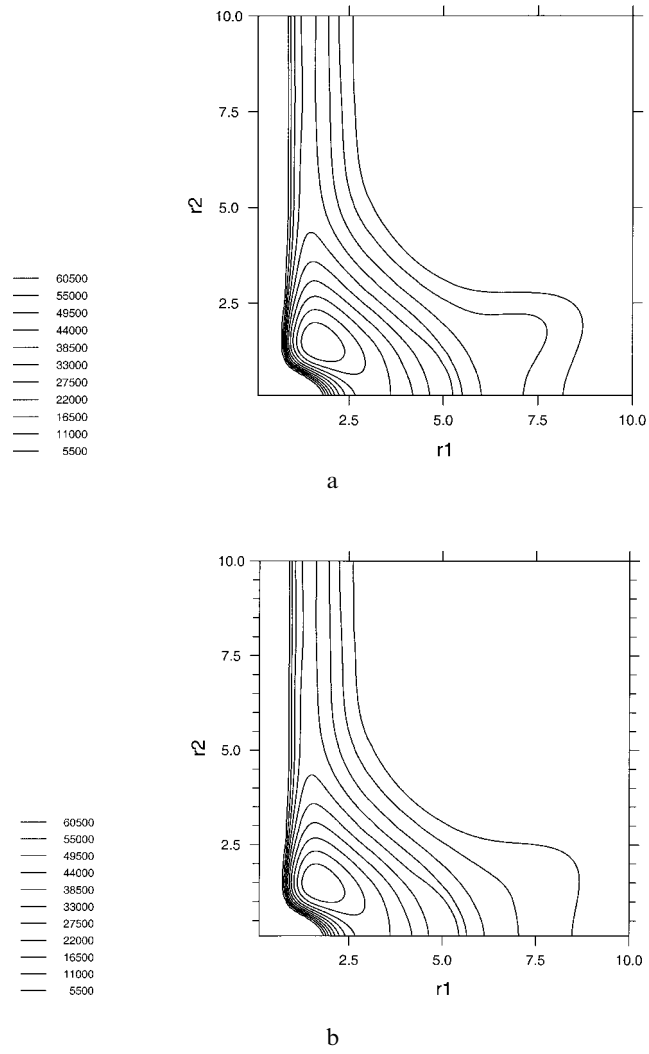

Figure 1. Contours of the H_3^+ potential energy surface in Jacobi coordinates with $\theta = 90^\circ$: (*a*) Fit 1 and (*b*) Fit 2.

Although the main goal of this work was to produce an accurate potential for energies up to $40\,000\,\mathrm{cm^{-1}}$, we thought it desirable to construct a potential which did not show this unphysical behaviour. As there were no *ab initio* points calculated in the region of the shoulder, it was not possible to just manipulate the weights of the points in the shoulder region to produce smoother behaviour. As an alternative, 100 artificial points were produced using the PPT potential. When these points were weighted equal to those of Schinke *et al.*, no significant change of the form of the potential was produced in the fit. It was necessary to increase the weighting of the points by a factor of four to be able to produce a relatively shoulder-free shape potential, see figure 1 (*b*). Other aspects of this fit were unchanged

from the previous one except that $R_{LIM} = 4.5\,a_0$ was used in equation (16).

This fit, Fit 2, represents a compromise between the form of the potential and the accuracy of the fit. The standard deviation with which Fit 2 reproduces the points of Cencek *et al.* and Schinke *et al.* increases by less than 10% to 0.069 cm^{-1} and 711 cm^{-1} respectively. As can be seen from table 1, Fit 2 represents the 115 of our points included in the fits with a standard deviation of 10.5 cm^{-1}, which is reduced to 6.9 cm^{-1} if the worst 5 points are discounted. Increasing the weight of the artificial points in the fit leads to significantly larger deterioration in the results, although the shape of the potential improved somewhat further. A full resolution of these problems must await the calculation of a much more extensive grid of high accuracy electronic structure points. Such a calculations is presently beyond our computer budget.

Tables 3–5 give our final parameters for the V_2 potential, the switching function and the V_1 potential respectively. Parameters for both Fit 1 and Fit 2 are presented. Potential parameters not specified here were frozen at the values of PPT for both fits. Fortran subroutines containing these potentials can be obtained from one of the authors (JT).

We consider Fit 2 to be the best compromise between the shape of the potential and the accuracy of the fit. In short, when accurate reproduction of the *ab initio* points is required, Fit 1 should be used. If the desired potential needs to be smooth at energies of 50 000 cm^{-1} or higher, Fit 2 should be used.

The surfaces we present are constructed within the Born–Oppenheimer approximation. Actually our treatment of the H_2 diatomic limit contains some allowance for adiabatic effects [33]. A proper treatment of adiabatic effects for the whole system would be of interest;

Table 3. Fitted coefficients for the V_2 Born–Oppenheimer potential, equation (7), in 10^{-6} atomic units. Errors, in the same units, are those given in the final iteration of the fit.

			Fit 1		Fit 2	
n	m	k	$V_{n,m,k}$	error	$V_{n,m,k}$	error
0	0	0	−0.400 00	0.0[a]	−0.400 00	0.0[a]
1	0	0	4.467 30	0.0[a]	4.467 29	0.0[a]
2	0	0	204 411.007 18	6.542 21	204 417.306 39	7.706 08
0	2	0	97 853.681 20	1.710 49	97 855.721 79	2.024 88
3	0	0	−49 416.182 13	27.117 44	−49 443.692 31	32.057 87
1	2	0	−235 073.540 99	10.852 51	−235 062.571 42	13.271 74
0	0	3	−32 823.035 09	2.681 27	−32 825.900 65	3.185 15
4	0	0	26 670.140 67	139.580 19	26 561.628 09	164.517 42
2	2	0	237 716.732 91	55.104 55	237 566.798 68	65.230 91
1	0	3	99 387.654 20	17.190 01	99 398.354 37	20.468 38
0	4	0	−760.066 93	9.979 24	−773.710 59	11.850 39
5	0	0	2 248.799 20	522.556 76	2 906.895 59	615.982 82
3	2	0	−146 180.296 74	194.265 92	−146 392.559 73	231.125 49
2	0	3	−130 013.625 50	63.388 33	−130 039.688 62	73.174 06
1	4	0	−13 130.504 35	58.123 48	−13 116.920 17	71.328 61
0	2	3	1 632.732 16	13.060 69	1 654.954 85	15.462 93
6	0	0	−10 984.105 67	1 100.920 51	−10 612.643 80	1 300.133 51
4	2	0	67 614.837 69	631.098 05	69 629.799 44	731.448 74
3	0	3	97 480.901 90	194.729 52	97 294.540 87	229.301 49
2	4	0	44 037.665 60	161.663 06	44 492.204 76	189.788 73
1	2	3	1 902.803 13	62.524 99	1 820.719 02	73.326 84
0	6	0	241.257 86	17.982 17	259.278 92	21.454 60
0	0	6	20.762 27	2.383 33	22.197 34	2.917 51
7	0	0	−33 576.699 19	3 312.431 49	−38 301.309 73	3 900.301 94
5	2	0	−21 488.782 63	1 502.532 22	−21 770.628 36	1 774.474 77
4	0	3	−56 328.317 80	616.601 61	−56 386.817 69	715.786 15
3	4	0	−62 205.948 19	722.466 83	−62 114.281 16	852.533 39
2	2	3	−18 233.711 27	292.421 45	−17 951.859 32	343.426 85
1	6	0	−2 118.627 57	115.022 22	−2 287.051 70	141.698 70
1	0	6	−1 178.768 26	17.907 63	−1 172.019 78	20.348 00

continued

Table 3. *Continued*

			Fit 1		Fit 2	
n	m	k	$V_{n,m,k}$	error	$V_{n,m,k}$	error
0	4	3	0.541 90	0.490 16	−48.567 40	24.119 92
8	0	0	75 158.195 43	4 488.886 19	76 486.267 73	5 303.295 18
6	2	0	37 795.302 10	2 854.223 72	29 251.591 30	3 283.991 66
5	0	3	61 665.888 44	1 019.879 25	65 239.578 46	1 145.121 70
4	4	0	69 885.589 19	1 169.188 26	65 706.681 88	1 321.930 57
3	2	3	43 380.857 30	362.805 90	42 544.580 04	401.793 69
2	6	0	5 273.175 78	247.291 32	5 122.497 54	298.617 39
2	0	6	4 040.641 11	43.890 40	3 947.616 29	42.752 78
1	4	3	−429.724 94	83.231 49	−169.054 63	93.983 03
0	8	0	−133.612 75	11.049 20	−119.993 90	13.284 72
0	2	6	1.355 32	0.602 19	8.238 89	4.551 46
9	0	0	82 487.068 03	8 173.053 45	95 599.814 46	9 620.024 89
7	2	0	−43 553.747 10	5 547.795 97	−35 124.308 26	6 398.057 17
6	0	3	−54 784.526 49	1 879.081 53	−56 206.204 70	2 206.683 17
5	4	0	−78 239.034 41	2 307.694 08	−75 825.866 06	2 747.042 99
4	2	3	−55 920.500 22	1 096.872 48	−56 210.749 91	1 298.139 25
3	6	0	−4 552.838 92	754.456 41	−3 657.320 20	889.592 21
3	0	6	−6 113.435 98	71.504 62	−6 198.674 71	83.259 97
2	4	3	998.651 82	343.834 96	520.228 15	404.975 24
1	8	0	1 275.893 97	76.212 23	1 380.664 65	93.122 52
1	2	6	564.111 15	26.784 05	520.228 15	32.316 22
0	6	3	35.504 57	10.494 38	62.455 89	12.315 23
0	0	9	−1.471 69	0.625 63	0.387 37	0.229 29
10	0	0	−164 462.751 26	9 437.382 32	−172 799.660 23	11 134.794 24
8	2	0	−45 557.050 60	4 523.739 15	−36 825.643 08	5 314.295 40
7	0	3	−42 858.636 89	2 219.703 54	−53 125.617 63	2 524.673 19
6	4	0	−25 696.207 04	4 277.865 86	−17 514.937 75	4 894.206 39
5	2	3	−25 241.907 65	2 667.246 84	−26 846.724 27	3 004.361 25
4	6	0	−6 357.229 75	1 906.184 61	−4 661.552 92	2 240.895 01
4	0	6	4 953.057 23	344.404 18	5 611.982 60	349.806 58
3	4	3	2 597.156 88	906.772 83	4 328.871 50	1 061.596 56
2	8	0	−1 997.367 41	250.936 48	−2 381.056 63	304.447 76
2	2	6	−1 855.784 30	93.073 63	−1 772.154 67	108.042 88
1	6	3	180.321 70	56.501 61	−44.807 34	64.173 61
1	0	9	20.358 34	3.304 62	12.559 49	3.698 56
0	10	0	9.676 88	2.395 49	−10.768 57	2.969 32
0	4	6	−11.046 59	1.319 01	−24.517 41	1.639 28
11	0	0	−65 222.142 70	6 742.538 03	−77 658.373 97	7 936.372 52
9	2	0	47 356.152 20	8 121.034 22	30 189.194 83	9 235.540 50
8	0	3	85 983.939 16	2 798.065 38	89 665.675 96	3 226.296 70
7	4	0	174 677.722 09	5 239.260 22	165 258.924 21	6 074.079 72
6	2	3	137 109.945 84	3 272.302 61	149 053.561 26	3 696.428 99
5	6	0	31 232.405 86	2 219.874 54	26 585.899 13	2 559.718 47
5	0	6	−4 630.579 65	518.295 40	−4 964.277 08	538.903 20
4	4	3	258.289 23	58.750 94	−3 568.701 84	1 220.936 71
3	8	0	−599.578 83	355.648 94	−477.371 00	426.204 07
3	2	6	2 685.260 47	135.601 87	2 491.674 43	153.788 12
2	6	3	−1 672.088 79	99.811 54	−1 247.473 65	111.594 04
2	0	9	−89.133 97	5.789 96	−75.454 74	6.261 32
1	10	0	−162.619 52	7.334 97	−94.898 64	9.281 44
1	4	6	−91.490 30	3.950 21	−47.106 83	4.908 31
0	8	3	−15.375 16	0.365 78	−11.758 51	0.480 37
0	2	9	0.058 63	0.000 32	0.060 82	0.000 46

continued

Table 3. *Continued*

			Fit 1		Fit 2	
n	m	k	$V_{n,m,k}$	error	$V_{n,m,k}$	error
12	0	0	124 146.605 20	7 454.185 35	134 500.715 47	8 784.680 82
10	2	0	15 877.504 19	5 296.350 78	22 995.791 86	6 092.666 01
9	0	3	−25 014.160 01	1 747.415 42	−18 268.522 01	2 063.490 40
8	4	0	−109 293.061 90	2 678.779 66	−106 740.696 69	3 121.790 50
7	2	3	−86 910.195 11	1 653.193 59	−97 386.244 70	1 890.805 30
6	6	0	−28 677.783 65	1 124.792 47	−26 501.646 27	1 282.240 97
6	0	6	3 835.998 15	271.470 19	3 603.483 89	296.310 65
5	4	3	−5 561.013 38	501.583 03	−3 062.226 78	573.626 40
4	8	0	1 802.448 31	181.659 18	2 014.536 12	216.319 63
4	2	6	−1 822.140 64	70.159 23	−1 502.767 59	78.533 50
3	6	3	1 778.567 54	56.565 26	1 549.979 87	62.584 64
3	0	9	79.981 59	3.292 64	71.567 41	3.467 19
2	10	0	190.930 78	5.544 51	138.506 48	7.113 94
2	4	6	135.028 64	2.933 55	100.760 83	3.636 32
1	8	3	19.478 17	0.459 19	14.955 40	0.603 21

[a] Constant held fixed in final iteration of fit.

Table 4. Parameters used to determine the switching function $f^{\pm}$, equation (3).

Parameter	Value
E_0/E_h	0.150 243 85
γ_0/E_h^{-1}	60.091 57
γ_1/E_h^{-3}	1.1×10^5

in particular, for the mixed isotopomers, it would require the introduction of extra dissociation channels.

4. Conclusions

We have produced an *ab initio* potential energy surface for the important and fundamental H_3^+ molecular ion within the Born–Oppenheimer approximation. This potential is expected to be accurate to a few reciprocal centimetres at all energies below the dissociation energy of the H_3^+ system and to be reliable at energies above this. Such a potential is necessary [16] if progress is to be made on the challenging problem of analysing the near-dissociation spectrum of H_3^+ recorded by Carrington and his co-workers [1–3].

Preliminary calculations performed using the empirically derived and less accurate PPT potential [18] suggest that the vibrational states supported by these potentials are somewhat different from those found in previous studies of H_3^+ vibrational states in the dissociating region [38]. The major reason for this appears to be the accurate treatment of long-range effects included in our new potentials which lead to much more attractive potentials as the ion dissociates. Our new potentials include these long-range effects. Nuclear motion calculations using the new potentials are in progress.

Alan Carrington's experiments have proved a continuing source of inspiration to us and we wish to dedicate this paper to him. We thank Sophie Kain for help with the figure and a referee for commenting on the adiabatic effects in the H_2 potential. This work has been supported by the Research Council of Norway (Programme for Supercomputing, Grant No. NN2694K) through a grant for computer time and the United Kingdom UK Engineering and Physical Sciences Research Council. The work of OLP is supported in part by the Russian Fund for Fundamental Studies. RP gratefully acknowledges a TMR Fellowship, under contract ERBFMBICT 960901. The research of WK has been made possible by a fellowship of the Royal Netherlands Academy of Arts and Sciences.

References

[1] CARRINGTON, A., BUTTENSHAW, J., and KENNEDY, R. A., 1982, *Molec. Phys.,* **45,** 753.
[2] CARRINGTON, A., and KENNEDY, R. A., 1984, *J. chem. Phys.,* **81,** 91.
[3] CARRINGTON, A., MCNAB, I. R., and WEST, Y. D., 1993, *J. chem. Phys.,* **98,** 1073
[4] CARRINGTON, A., and MCNAB, I. R., 1989, *Acc. Chem. Res.,* **22,** 218.
[5] MCNAB, I. R., 1994, *Adv. chem. Phys.,* **89,** 1.
[6] GOMEZ-LLORENTE, J. M., and POLLAK, E., 1987, *Chem. Phys. Lett.,* **138,** 125.
[7] PFEIFFER, R., and CHILD, M. S., 1987, *Molec. Phys.,* **60,** 1367.

Table 5. Parameters use to determine the short-range three-body term, $V_{aa}^{(3)SR}$, equations (11)–(13). Errors are those given in the final iteration of the fit.

	Fit 1		Fit 2	
Parameter	value	error	value	error
C_1/Å^{-1}	−0.578 58	0.001 98	−0.571 41	0.003 31
C_{11}/$^{-2}$	0.419 66	0.009 85	0.506 48	0.013 16
C_{12}	−1.321 17	0.010 31	−1.390 38	0.013 37
C_{111}/Å^{-3}	−0.250 80	0.024 78	−0.067 68	0.028 30
C_{112}	0.449 60	0.023 29	0.269 39	0.028 48
C_{123}	0.110 73	0.062 23	0.506 84	0.063 14
C_{1111}/Å^{-4}	−0.910 92	0.030 52	−1.112 17	0.031 09
C_{1112}	1.020 59	0.041 84	1.367 34	0.055 26
C_{1122}	0.101 77	0.075 04	−0.505 93	0.097 04
C_{1123}	−0.346 66	0.019 79	−0.293 97	0.029 91
C_{11111}/Å^{-5}	1.473 12	0.081 29	1.067 22	0.058 43
C_{11112}	−1.295 48	0.132 85	−0.703 64	0.094 68
C_{11122}	−0.327 08	0.040 73	−0.361 99	0.035 27
C_{11123}	0.941 18	0.320 35	−0.794 32	0.284 08
C_{11223}	−1.228 31	0.211 47	−0.077 24	0.211 49
C_{111111}/Å^{-6}	−0.686 53	0.042 60	−0.399 36	0.035 10
C_{111112}	0.364 78	0.095 32	0.097 88	0.070 16
C_{111122}	1.221 16	0.166 41	1.005 77	0.153 79
C_{111222}	−1.723 36	0.316 09	−1.435 04	0.274 44
C_{111123}	−0.748 27	0.485 26	−0.500 32	0.297 62
C_{111233}	0.862 29	0.454 16	1.142 22	0.293 98
C_{112233}	−2.253 44	1.321 98	−3.552 67	0.917 94
$C_{1111111}$ /Å^{-7}	0.063 88	0.011 49	0.013 63	0.007 35
$C_{1111122}$	−0.588 26	0.062 21	−0.477 22	0.039 64
$C_{1111112}$	0.160 07	0.022 11	0.176 97	0.016 99
$C_{1111123}$	−0.393 37	0.084 78	−0.352 02	0.075 25
$C_{1111222}$	0.361 43	0.054 32	0.289 53	0.032 19
$C_{1111223}$	0.283 91	0.051 97	0.201 80	0.078 10
$C_{1112223}$	−0.270 02	0.150 56	−0.294 58	0.099 51
$C_{1122333}$	0.109 65	0.095 93	0.170 27	0.059 86
V_0 [a]/eV	3.782 643			
R_0 [a]/Å	0.891 756			
g_1 [a]/Å^{-1}	0.820 040			

[a] Constant fixed at value determined by PPT [18] in both fits.

[8] BERBLINGER, M., POLLAK, E., and SCHLIER, C., 1988, *J. chem. Phys.,* **88,** 5643.

[9] BERBLINGER, M., GOMEZ-LLORENTE, J. M., POLLAK, E., and SCHLIER, C., 1988, *Chem. Phys. Lett.,* **146,** 353.

[10] CHAMBERS, A. V., and CHILD, M. S., 1988, *Molec. Phys.,* **65,** 1337.

[11] BERBLINGER, M., SCHLIER, C., and POLLAK, E., 1989, *J. chem. Phys.,* **93,** 2319.

[12] POLLAK, E., and SCHLIER, C., 1989, *Acc. Chem. Res.,* **22,** 223.

[13] GOMEZ-LLORENTE, J. M., ZAKRZEWSKI, J., TAYLOR, H. S., and KULANDER, K. C., 1988, *J. chem. Phys.,* **89,** 5959.

[14] POLAVIEJA, G. G., FULTON, N. G., and TENNYSON, J., 1994, *Molec. Phys.,* **83,** 361.

[15] POLAVIEJA, G. G., FULTON, N. G., and TENNYSON, J., 1996, *Molec. Phys.,* **87,** 651.

[16] HENDERSON, J. R., and TENNYSON, J., 1996, *Molec. Phys.,* **89,** 953.

[17] MANDELSHTAM, V. A., and TAYLOR, H. S., 1997, *J. chem. Soc. Faraday Trans.,* **93,** 847.

[18] PROSMITI, R., POLYANSKY, O. L., and TENNYSON, J., 1997, *Chem. Phys. Lett.,* **273,** 107.

[19] VARANDAS, A. J. C., 1996, *J. chem. Phys.,* **105,** 3524.

[20] DINELLI, B. M., POLYANSKY, O. L., and TENNYSON, J., 1995, *J. chem. Phys.,* **103,** 10433.

[21] SCHINKE, R., DUPUIS, M., and LESTER JR, W. A., 1980, *J. chem. Phys.,* **72,** 3909.

[22] CENCEK, W., RYCHLEWSKI, J., JAQUET, R., and KUTZELNIGG, W., 1998, *J. chem. Phys.,* **108,** 2831.

[23] MEYER, W., BOTSCHWINA, P., and BURTON, P. G., 1986, *J. chem. Phys.,* **84,** 891.

[24] KUTZELNIGG, W., 1985, *Theor. Chim. Acta,* **68,** 445.

[25] KLOPPER, W., and KUTZELNIGG, W., 1987, *Chem. Phys. Lett.,* **134,** 17.
[26] KLOPPER, W., and RÖHSE, R., 1992, *Theor. Chim. Acta,* **83,** 441.
[27] RÖHSE, R., KLOPPER, W., and KUTZELNIGG, W., 1993, *J. chem. Phys.,* **99,** 8830.
[28] RÖHSE, R., KUTZELNIGG, W., JAQUET, R., and KLOPPER, W., 1994, *J. chem. Phys.,* **101,** 2231.
[29] RÖHSE, R., and KLOPPER, W., 1993, DIS, a CISD-R12 program for two-electron molecular systems.
[30] POLYANSKY, O. L., and TENNYSON, J., 1999, *J. chem. Phys.,* **110,** 5056.
[31] MURRELL, J. N., CARTER, S., FARANTOS, S. C., HUXLEY, P., and VARANDAS, A. J. C., 1984, *Molecular Potential Energy Functions* (New York: Wiley).
[32] CARTER, S., 1983, unpublished results (see [31], Chap. 11).
[33] BISHOP, D. M., and SHIH, S.-K., 1976, *J. chem. Phys.,* **64,** 162.
[34] SCHWARTZ, C., and LE ROY, R. J., 1987, *J. molec. Spectrosc.,* **121,** 420.
[35] GIESE, C. F., and GENTRY, W. R., 1974, *Phys. Rev.* A, **10,** 2156.
[36] LAW, M. M., and HUTSON, J. M., 1997, *Comput. Phys. Comm.,* **102,** 252.
[37] COSBY, P. C., and HELM, H., 1988, *Chem. Phys. Lett.,* **152,** 71.
[38] PROSMITI, R., MUSSA, H. Y., and TENNYSON, J., 1998, *Molecular Quantum States at Dissociation*, edited by R. Prosmiti, J. Tennyson and D. C. Clary (Daresbury, UK: CCP6).